

## PAPER

## Novel flexible Parylene neural probe with 3D sheath structure for enhancing tissue integration

Cite this: *Lab Chip*, 2013, 13, 554

Jonathan T.W. Kuo,<sup>a</sup> Brian J. Kim,<sup>a</sup> Seth A. Hara,<sup>a</sup> Curtis D. Lee,<sup>a</sup> Christian A. Gutierrez,<sup>c</sup> Tuan Q. Hoang<sup>a</sup> and Ellis Meng<sup>\*ab</sup>

A Parylene C neural probe with a three dimensional sheath structure was designed, fabricated, and characterized. Multiple platinum (Pt) electrodes for recording neural signals were fabricated on both inner and outer surfaces of the sheath structure. Thermoforming of Parylene was used to create the three dimensional sheath structures from flat surface micromachined microchannels using solid microwires as molds. Benchtop electrochemical characterization was performed on the thin film Pt electrodes using cyclic voltammetry and electrochemical impedance spectroscopy and showed that electrodes possessed low impedances suitable for neuronal recordings. A procedure for implantation of the neural probe was developed and successfully demonstrated *in vitro* into an agarose brain tissue model. The electrode-lined sheath will be decorated with eluting neurotrophic factors to promote *in vivo* neural tissue ingrowth post-implantation. These features will enhance tissue integration and improve recording quality towards realizing reliable chronic neural interfaces.

Received 16th August 2012,  
Accepted 22nd October 2012

DOI: 10.1039/c2lc40935f

[www.rsc.org/loc](http://www.rsc.org/loc)

### Introduction

Reliable and robust brain machine interfaces (BMI) that enable direct patient control of motor prosthetics are an ongoing challenge. Electrophysiological methods to communicate and probe the nervous system have been explored extensively since the discovery in the 18th century that electrical signals modulate muscle movements.<sup>1</sup> Implantable probes with single or arrays of neural recording and stimulation electrodes, simply referred to sometimes as “neural probes”, that reliably interact and communicate with neurons have served as standard neuroscience research tools for studies of brain function for decades but have yet to achieve their potential in clinical use. Individuals with neurodegenerative disorders or other neurological deficits may benefit from neural probe technologies to restore brain function lost by disease (stimulating electrodes) or re-establish previously severed brain-limb connections as in limb control (recording electrodes).

Earlier BMI technology consisted of individual metal microwires (>75  $\mu\text{m}$  diameter)<sup>2</sup> with de-insulated tips for recording neural signals.<sup>3</sup> Later, arrays of microwires held together with adhesive led to improved spatiotemporal neural

recordings.<sup>4</sup> With the emergence of microfabrication technologies, silicon (Si) shanks supporting patterned microelectrodes were developed for use as neural probes; today, two probe types are prevalent. The Michigan probes, introduced in 1986, consists of Si micromachined probes with multiple electrode recording sites patterned along the shank (later commercialized by NeuroNexus).<sup>5</sup> The Utah probe array, introduced shortly thereafter, consists of arrays of Si micromachined shanks each with an individual metal recording site located at the shank tip (later commercialized by Blackrock Microsystems).<sup>6</sup> Dense arrays of recording sites are possible with either technology platform.

Despite many decades of development, however, current implanted neural probes possess short recording lifetimes; reliable neural recordings are typically obtained in durations measured in months. This short lifetime is attributed to the physiological response of surrounding neural tissue to the implanted neural probe.<sup>7</sup> Upon implantation, brain micromotion due to blood flow, respiration, and head movement aggravates the tissue surrounding the device and a physiological response begins that involves inflammation, glial scar encapsulation of implant, and retraction of neurons from recording sites leading to a loss of recordable neural signal. One contributing factor for tissue aggravation is the mechanical mismatch in elastic moduli between the stiff probe material and surrounding soft neural tissue. Microwires made of noble metals or micromachined Si shanks (Young's modulus,  $E \sim 100\text{--}400$  GPa) possess Young's moduli many orders higher than neural tissue ( $E \sim 0.1\text{--}6$  kPa).<sup>8</sup> A chronic strain is induced on the probe-tissue interface upon implanta-

<sup>a</sup>Department of Biomedical Engineering, University of Southern California, 1042 Downey Way, DRB-140, Los Angeles, CA, 90089-1111, USA.

E-mail: [ellis.meng@usc.edu](mailto:ellis.meng@usc.edu); Fax: +1-213-821-3897; Tel: +1-213-740-6952

<sup>b</sup>Ming Hsieh Department of Electrical Engineering, University of Southern California, 3740 McClintock Ave., EEB-100, Los Angeles, CA, 90089-2560, USA.

E-mail: [ellis.meng@usc.edu](mailto:ellis.meng@usc.edu); Fax: +1-213-821-3897; Tel: +1-213-740-6952

<sup>c</sup>Los Angeles, CA 90089-2560, USA

tion with resulting shear forces scaling with the moduli difference between probe and tissue.<sup>9</sup> Besides the material mechanical mismatch, the common practice of anchoring the implanted neural probe to a stationary object such as the skull also increases tissue aggravation since the skull-anchored probe opposes natural brain micromotion.

A neural probe technology which has achieved long recording lifetime (in both animals and humans) measured in years is the neurotrophic cone electrode.<sup>10–16</sup> This non-micromachined technology is fundamentally different from other microwire or silicon-based neural probes. The long term success of the neurotrophic cone electrode is attributed to its use of growth factors and its hollow structure. The overall structure is based on a glass cone formed by pulling a heated pipette and then cutting to achieve the desired length (1–2 mm). Microwires are then manually positioned within the cone and glued into place. Next, growth factors that promote neural tissue growth such as Matrigel and nerve growth factor (NGF) are coated within the cone prior to implantation. The release of factors *in vivo* is thought to attract neural tissue growth into the cone towards the microwire recording sites. The ingrowth of neural tissue into the cone mechanically integrates and anchors the probe to the tissue; thus the detrimental effects of brain micromotion are minimized by reducing chronic strain at probe-tissue interface. The ingrowth of neural processes into the cone toward recording sites leads to better neural signal recording since the distance between neuron and recording site is minimized.

Unlike silicon probes, neurotrophic cone electrodes are individually assembled using a manual labor intensive process that is prone to low yield, throughput, and probe–probe

repeatability. Glass ( $E \sim 100$  GPa) still poses a mechanical mismatch issue with neural tissue. Finally, microwire spatial requirements limit the number of recording sites possible per cone; a maximum of four recording sites per cone electrode was demonstrated.

To overcome manufacturing and electrode density limitations of cone electrodes that prevent its widespread use, a batch fabricated Parylene flexible neural probe using a novel process that enables a three dimensional (3D) sheath structure was developed.<sup>17</sup> Microfabrication technologies allow for precise patterning of multiple recording electrodes per sheath (eight electrodes for this device; Fig. 1). Electrodes can be placed on both inner and outer surfaces of the sheath. Batch fabrication ensures high throughput with repeatability of dimensions and high fidelity of characteristics and behaviors throughout multiple probes. A post-fabrication thermoforming process is used to obtain the final 3D structure and open the lumen of the sheath. The lumen can accommodate neurotrophic factor coatings and allows for tissue ingrowth upon implantation thereby anchoring the neural probe to tissue and improving its recording by attracting neural processes to interior recording sites. Coatings of eluting anti-inflammatory factors may also be applied to the sheath to mitigate inflammatory and encapsulation processes in the surrounding tissue.

## Methods

Parylene C, a micromachinable and FDA-approved USP class VI biocompatible polymer,<sup>18,19</sup> was selected as the structural

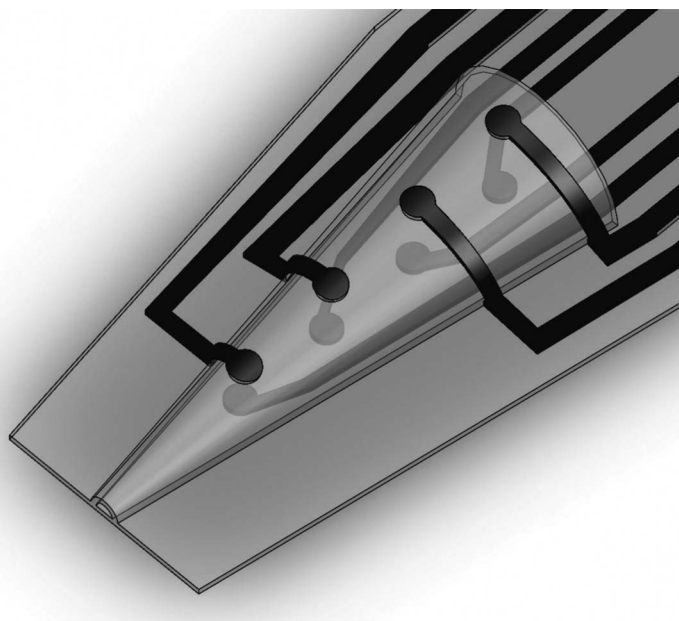


**Fig. 1** Parylene neural probe with 3D sheath structure. The sheath structure allows for ingrowth of neural processes leading to improved tissue/probe integration post implantation. The sheath interior can be coated with neurotrophic factors to promote ingrowth and attract processes to recording sites for improved recording quality and longevity. Eight Pt recording electrodes per sheath probe are patterned, four on the sheath interior and four on the exterior.

material for the 3D sheath structure and cable substrate as it improves upon the mechanical mismatch between neural probe and neural tissue since ( $E \sim 4$  GPa is an order of magnitude lower than glass and silicon<sup>20</sup>). Platinum (Pt), a highly inert and biocompatible metal,<sup>18</sup> was selected as the recording electrode material. Pt is a common material used for neural electrodes and preferred over other metals since it is known to be inert under biological environments and possesses a high charge injection limit.<sup>21</sup> Also no adhesion layer is required when depositing Pt onto Parylene substrate.<sup>22</sup> First, surface micromachining techniques were used to define the initially flat Parylene neural probe structure (Fig. 2). A bare Si wafer with its native oxide layer was used as a carrier substrate during the microfabrication process. The native oxide facilitates release of the Parylene probe from the wafer surface at the conclusion of the surface micromachining process. A base layer of 5  $\mu\text{m}$  Parylene (Parylene C, Specialty Coating Systems, Indianapolis, IN) was first deposited onto a dehydration baked (120  $^{\circ}\text{C}$ , 20 min) Si wafer. Pt metal electrodes, leads, and contact pads were patterned, e-beam deposited (2000  $\text{\AA}$ ), and liftoff processed to create recording

sites located on the sheath interior. Next, an insulation layer of Parylene (1  $\mu\text{m}$ ) was deposited, patterned, and  $\text{O}_2$  plasma etched (100 W, 100 mT) to expose the recording sites and contact pads. A thick photoresist, AZ 4620 (AZ Electronic Materials, Branchburg, NJ) was spun on (9.6  $\mu\text{m}$ ) and patterned; this serves as the sacrificial material for the Parylene microchannel which eventually becomes the 3D sheath. 5  $\mu\text{m}$  Parylene was deposited over the sacrificial photoresist creating the microchannel. A dual layer photoresist liftoff scheme (AZ 1518/AZ 4620; AZ Electronic Materials, Branchburg, NJ) was utilized to pattern outer sheath electrodes located on top of the microchannel. The dual layer photoresist scheme was necessary to ensure trace continuity across the microchannel following liftoff.<sup>23</sup> Another Parylene insulation layer (1  $\mu\text{m}$ ) was deposited and plasma etched to expose the outer electrodes and contact pads. Microchannel openings and the neural probe outline were plasma etched. An acetone soak followed by an isopropyl alcohol rinse removed any remaining photoresist and released the microchannels. Finally, the Parylene neural probe was released from the wafer by applying a gentle lifting force with tweezers with the wafer submerged in DI water.

A custom fabricated tungsten (MicroProbes for Life Science, Gaithersburg, MD) or stainless steel microwire (Cooner Wire Co., Chatsworth, CA) matching the desired probe shape was carefully inserted into the microchannel opening using a microscope (Fig. 3). The apparatus was then held in a custom made aluminum jig and placed into a vacuum oven (Laboratory Vacuum Oven Model V0914A, Lindberg/Blue,

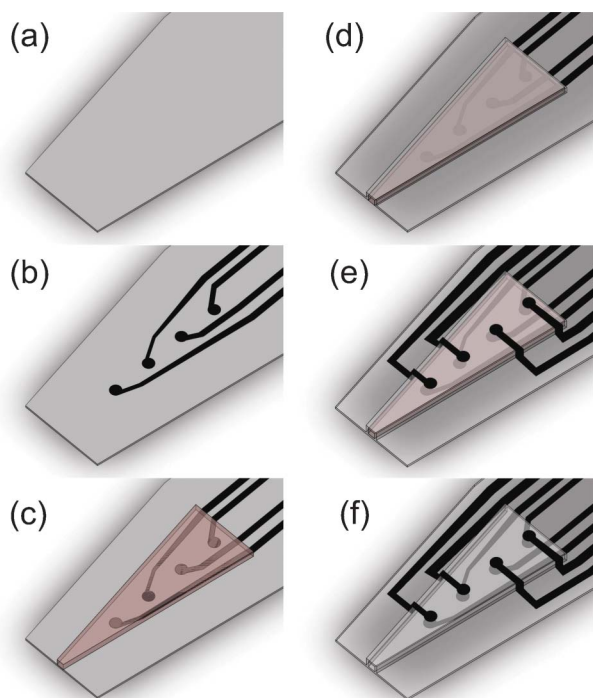


**Fig. 2** Fabrication process of the Parylene neural probe. (a) Base layer of 5  $\mu\text{m}$  Parylene was deposited onto a bare Si wafer. (b) Pt recording electrodes were patterned onto the wafer by liftoff. Another 1  $\mu\text{m}$  Parylene insulation layer was deposited and recording sites and contact pads were patterned and plasma etched. (c) Sacrificial photoresist was patterned to create the desired microchannel shape. (d) A 5  $\mu\text{m}$  Parylene layer was deposited over the sacrificial photoresist. (e) Pt recording electrodes were patterned atop the microchannel and a 1  $\mu\text{m}$  Parylene insulation layer was deposited and plasma etched to open the recording sites and contact pads. (f) Openings in the microchannel as well as the device cutout were plasma etched. The sacrificial photoresist was removed with an acetone soak. The Parylene microchannel is now ready for the thermoforming process which creates the final 3D sheath structure.

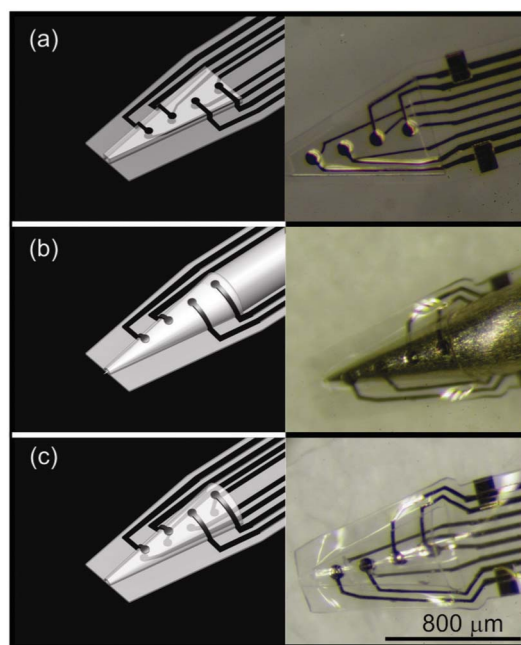


**Fig. 3** Thermoforming process. (a) Thermoforming commenced following the surface micromachining process. (b) A microwire was inserted into the microchannel and the assembly was thermoformed. (c) After thermoforming, the microwire mold was removed and the three dimensional sheath was retained in the final structure.

Asheville, NC) for thermoforming to produce the final 3D sheath shape. Although this process was performed on individual sheaths, this technique is easily extended to linear sheath arrays with corresponding microwire arrays.

Parylene is a thermoplastic that can be thermoformed with a mold to transform its as-fabricated shape.<sup>24,25</sup> The thermoforming process takes place at 200 °C (well above Parylene's glass transition temperature of  $\sim 90$  °C<sup>26</sup>), results in increased crystallinity of the polymer, and allows the thermoplastic film to take on the shape of the mold even after the mold is removed. Parylene sheaths can thus be obtained by thermoforming following the surface micromachining process (Fig. 3). Thermoforming was performed under vacuum to prevent Parylene oxidative degradation. Nitrogen purging was used to minimize oven oxygen content. The probes were annealed under vacuum at 200 °C for 48 h. After cooling to room temperature, the microwire was easily removed without the assistance of any release coatings.

External electrical connections with electrodes were established using zero-insertion-force (ZIF) connectors (HIROSE Electric USA, Inc., Simi Valley, CA).<sup>27</sup> A polyetheretherketone (PEEK) polymer sheet (8504K13, McMaster-Carr, Aurora, OH) cut out to match contact pad area was applied behind the Parylene substrate with cyanoacrylate adhesive (Instant Crazy Glue, Elmer's Products, Inc., Westerville, OH) to stiffen the flexible cable assembly and match the required cable thickness for the ZIF interface. The stiffened contact pad region was inserted into the ZIF connector, the connector pins aligned, and the cable lock flipped into place (Fig. 4). It should be noted that the electrical connector assembly is not implanted and so material biocompatibility is not strictly required.

The neural probe was electrochemically characterized using electrochemical impedance spectroscopy (EIS) and cyclic voltammetry (CV). Electrodes were connected to a potentiostat (Reference 600, Gamry Instruments, Warminster, PA) using the ZIF interface and placed in a Faraday cage (VistaShield

Faraday Cage; Gamry Instruments, Warminster, PA) to minimize ambient electrical noise. For EIS, probes were immersed in 1× phosphate buffer solution (PBS; OmniPur 10× PBS, EMD Chemicals, Darmstadt, Germany) with a separate Ag/AgCl reference electrode (RE-5B Ag/AgCl Reference Electrode, BASi, West Lafayette, IN). Impedances were recorded over 1 Hz to 100 kHz. CV was performed by immersing probes in 0.05 M sulfuric acid (EMD Chemicals, Darmstadt, Germany) along with an Ag/AgCl reference electrode. One probe electrode was set as the working electrode while an adjacent Pt electrode served as the counter. Voltage was cycled between  $-0.2$  to  $1.2$  V with a scan rate of  $250$  mV s<sup>-1</sup>. 50 scans were taken to ensure a stable voltammogram was obtained and recorded.

Polymer neural probes were designed to be compliant in order to minimize brain tissue aggravation upon implantation. This compliance poses a problem during probe implantation since the probe may buckle while attempting to penetrate neural tissue. Compliant probes may also deflect during implantation and miss the target neural area. Techniques to temporarily stiffen polymer probes during implantation have been investigated and involve coating or filling with biodegradable polymers that dissolve *in vivo*<sup>2,28</sup> or attaching to stiff shuttles that are removed after implantation.<sup>29</sup>

A procedure for surgical placement of individual probes was developed and made use of a custom introducer tool consisting of a stainless steel or tungsten microwire attached to a Si support plate. The microwire was aligned to the sheath under a microscope and inserted into the sheath. Polyethylene glycol (PEG; MW 8000, Sigma-Aldrich, St. Louis, MO), a biodegradable polymer, was melted at 90 °C and transferred by pipette to temporarily adhere the probe to the microwire. PEG is biocompatible, water soluble, and was used as a temporary adhesive during neural implantations.<sup>2,28</sup> PEG was

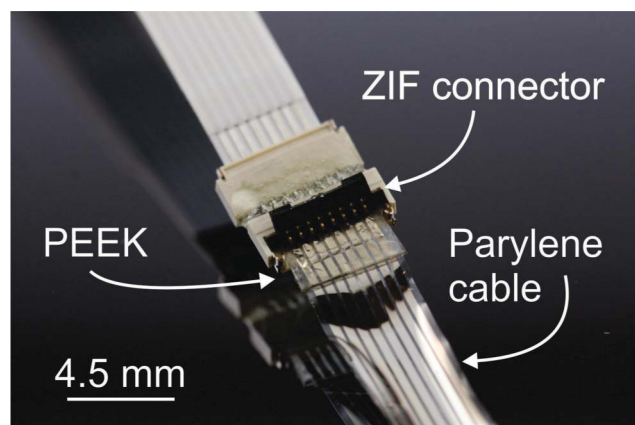


**Fig. 4** Electrical packaging scheme for the fabricated Parylene sheath neural probe. PEEK was attached to the back of the Parylene contact pads with cyanoacrylate adhesive to serve as a stiffener material. The contact pads were inserted into the ZIF connector and the pins were aligned to the contact pads. The flip lock was secured to complete the electrical connection.

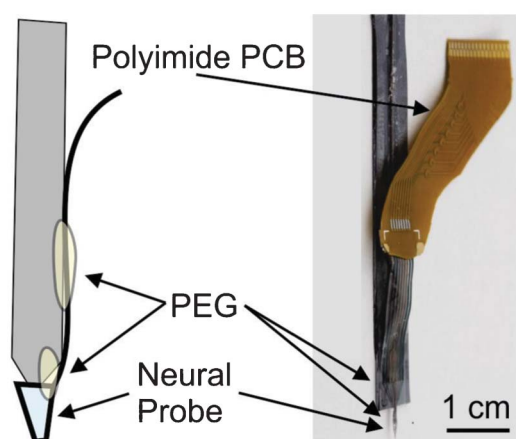


**Fig. 5** Surgical introducer tool for sheath neural probe. The introducer tool consisted of a microwire attached to a flat silicon support. The microwire was inserted into the micromachined Parylene sheath structure and PEG was applied as a temporary adhesive. PEG was also applied to temporarily adhere the Parylene cable to the introducer tool. The probe shown in the photograph on the right was attached via ZIF interface to a polyimide flexible printed circuit board which interfaced to electrophysiological recording equipment.



also used to temporarily connect the Parylene cable to the introducer tool (Fig. 5). The introducer tool with the attached sheath probe was placed onto a stereotaxic frame.

An agarose (A9539-50G, Sigma-Aldrich, St. Louis, MO) gel block (0.5%) was prepared as a brain tissue model. Agarose is widely used within the neuroscience community to mimic the biomechanical viscoelastic properties of neural tissue since 0.5% agarose possesses similar elastic and shear moduli.<sup>29</sup> Using the stereotaxic frame, the probe was positioned over the agarose and slowly lowered. Since the intended targets for these probe designs are the cortical layers in rat barrel cortex at 2 mm depth, the probe was inserted 2 mm into the agarose, as measured by the built-in micrometer.

The sheath probe and cable were released by dissolving the temporary PEG adhesive using saline solution applied by a syringe. After a short wait period (up to 5 min) to ensure complete dissolution, the introducer tool was retracted using the stereotaxic frame.

## Results and discussion

Parylene sheath neural probes were fabricated with each probe possessing eight Pt recording electrodes of 45  $\mu\text{m}$  diameter; four electrodes each were linearly arranged and evenly spaced along the interior and exterior of the sheath over a length of 800  $\mu\text{m}$  (Fig. 6). An electrode surface area of  $\sim 1500 \mu\text{m}^2$  was chosen to maximize neural recording while minimizing cross-talk and impedance.<sup>30</sup> Successful electrical connection to recording electrodes using the ZIF interface was confirmed with a multimeter (2700 MultiMeter, Keithley Instruments Inc., Cleveland, OH). Lead impedances ranging 325–389  $\Omega$  were found demonstrating that the dual photoresist liftoff scheme was successful in patterning continuous leads from the base of the sheath structure to the top.

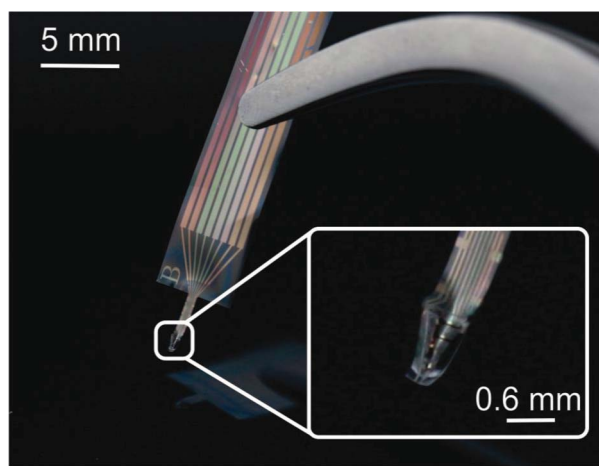
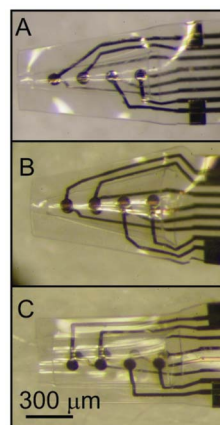


**Fig. 6** Fabricated flexible Parylene sheath neural probe with integrated Parylene cable. The thermoformed 3D sheath structure is clearly seen at the neural probe end of the device.



Design	Probe Openings	
	Tip [ $\mu\text{m}$ ]	Base [ $\mu\text{m}$ ]
A	50	300
B	50	450
C	300	300

**Fig. 7** Fabricated sheath probe design variations. 45  $\mu\text{m}$  diameter Pt electrodes were patterned for all devices. All designs spanned a length of 800  $\mu\text{m}$  to fully capture neural signals in targeted multiple cortex layers upon implantation. Designs A and B feature sheath structures with different tapers while design C possesses a cylindrical structure.

Different sheath shapes and designs were fabricated for future *in vivo* studies to determine the effect of sheath dimension on neural tissue ingrowth as it is currently unknown whether different neural probe shapes will affect the reliability of long-term neural recordings (Fig. 7). Design A dimensions were selected to closely match those of the neurotrophic cone electrode. A sheath with a wider taper was also fabricated in design B. In design C, a cylindrical sheath structure was fabricated. For all sheath probe variations, the recording electrodes were spaced equidistantly along the length of the sheath structure (800  $\mu\text{m}$ ) to fully span and record from the rat barrel cortex layers IV–VI.

Thermoforming with a microwire mold produced consistent 3D sheath structures. SEM micrographs of the sheath structures taken a week after the thermoforming procedure demonstrated that structures maintained their shape and did not sag or otherwise revert to the original flat microchannel shape (Fig. 8). Thermoforming at 200  $^{\circ}\text{C}$  also served to anneal the multiple Parylene layers leading to improved Parylene/Parylene adhesion<sup>31–33</sup> and improved sheath probe mechanical robustness. Improved mechanical robustness of the sheath probe was confirmed using a nanoindenter (Berkovich tip, MTS Nano Indenter XP) to determine stiffness of the sheath structure. The cone structure stiffness increased up to 60 times following a thermoforming process (compared to an as-fabricated sample), and returned to its original shape following deformation with a fine-tipped probe (data not shown).

The method of manual insertion of a microwire into the microchannel structure is potentially labor intensive and can pose a throughput issue. However, this limitation can easily be overcome by patterning the neural probes on the wafer such that they are spaced with a defined distance. An array of microwires in which the spacing between microwires matches the defined distance of the microchannel openings can then

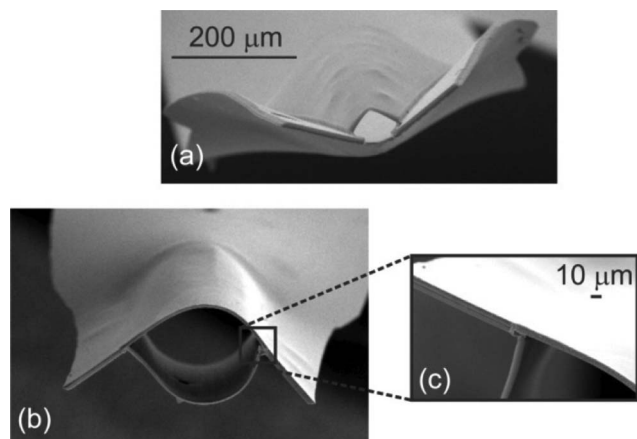


**Fig. 8** SEM imaging of thermoformed Parylene sheath structures taken a week post-thermoforming. A conical sheath structure (a), a cylindrical sheath (b), and a close up of the interface between the Parylene layers that define the sheath (c) are presented. Thermoforming of Parylene creates structures that hold their shape indefinitely; the Parylene does not revert to its original microchannel geometry.

be used to insert many microwire molds into multiple microchannels in one step. Then mold-mounted probes can be thermoformed simultaneously in large quantities.

Electrical packaging of the sheath probes with ZIF connectors was verified by successful electrochemical characterization. Electrical signals from the Pt recording electrodes transmitted successfully through the leads in the Parylene cable through the ZIF connector to the potentiostat and were recorded. ZIF to Parylene connections are mechanically robust and were demonstrated to withstand loads up to 120 g without failure.<sup>27</sup>

These connections are reversible, reusable, and amenable to scaling since multiple electrical connections are made or broken at once by engaging or disengaging, respectively, the cable lock. In contrast, traditional wire bonding and conductive epoxy methods are permanent, can be labor intensive, and may suffer from low yield when contacts must be manually established.

Electrochemical characterization of the electrodes confirmed that the fabricated sheath probe possessed desirable characteristics for successful neural recordings. EIS of the electrodes revealed impedances of 20–60 k $\Omega$  at 1 kHz. Impedances of less than 1 M $\Omega$  are desirable for neural recording<sup>30</sup> and lower impedances portend neural recording success upon implantation (Fig. 9).<sup>34</sup> CV of the Pt electrodes immersed in sulfuric acid resulted in voltammograms that matched the classic electrochemical response of bulk Pt in sulfuric acid. Hydrogen adsorption and desorption peaks were observed as well as peaks from the formation and reduction of Pt oxide (Fig. 10). This demonstrates that thin film Pt electrodes possess the same electrochemical properties as bulk Pt and can be reasonably expected to possess the same recording capabilities as traditional Pt microwires used for neural recording.

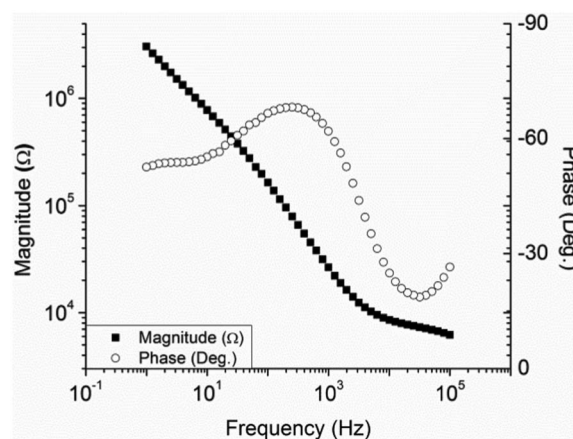


**Fig. 9** Representative EIS of a Pt electrode.

*In vitro* insertion of the neural probe into the brain tissue model was successful. Upon release of the device from the introducer tool and microwire, the neural probe remained embedded in the agarose solution as the introducer tool was retracted (Fig. 11). The implanted neural sheath probe did not collapse, remained in its target insertion depth of 2 mm, and did not change position based on visual inspection (data not shown).

The Parylene sheath probes represent an improvement over neurotrophic glass cone electrode technology. Parylene batch microfabrication ensures probe-to-probe repeatability with multiple recording electrodes placed on sheath lumen as well as outer surfaces in contrast to the individual assembly of neurotrophic cone electrodes with a limited number of recording sites. Parylene is much more compliant than glass and so alleviates mechanical mismatch. Like the cone

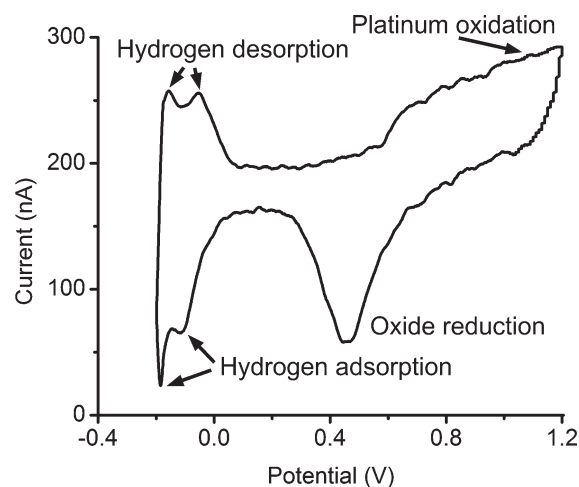


**Fig. 10** Representative voltammogram of a Pt electrode immersed in sulfuric acid. Hydrogen adsorption and desorption peaks as well as Pt oxide formation and reduction peaks were clearly seen. The recorded voltammogram matched that of bulk Pt in sulfuric acid.

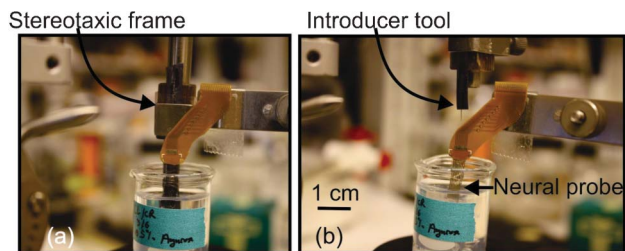


**Fig. 11** *In vitro* implantation of fabricated neural probe using the introducer tool was successful. (a) The neural probe attached to the introducer tool with PEG was first lowered into agarose gel with a stereotaxic frame. (b) Upon release of neural probe from the introducer tool by dissolution of PEG, the introducer tool was raised out of the agarose while the neural probe remained implanted in the brain tissue model.

electrodes, the 3D sheath structures can accommodate growth factor and anti-inflammatory coatings that elute and lead to ingrowth of neural tissue for improved tissue-probe mechanical anchoring. In this work, sheath probe dimensions were chosen to match the neurotrophic cone electrode; it is important to note that smaller dimensions are possible with the same fabrication process and are limited only by photolithographic resolution. For thermoforming, it is possible to custom etch tungsten microwires to match smaller sheath probe dimensions.<sup>35</sup>

## Conclusions

A Parylene neural probe with a 3D sheath structure for improved neural recordings and integration was designed and fabricated. A novel fabrication scheme was introduced in which a 3D hollow sheath structure was produced with multiple Pt recording electrodes on the interior and exterior using a combination of surface micromachining and thermoforming processes. Convenient and reusable electrical connections with flexible Parylene cables were achieved with ZIF connectors. Electrochemical characterization of the electrodes demonstrated desirable properties for neural recordings. A novel implantation method suitable for this probe architecture was developed and successfully demonstrated *in vitro* in a brain tissue model. The novel fabrication method presented in which flat surface micromachined structures can be modified post-fabrication to form 3D structures is not only an enabling technology for next generation neural probes but also has implications on flexible and 3D microfluidic platforms for fluid delivery or tissue ingrowth.

Current work includes development of deposition processes for decorating neurotrophic factors onto probe surfaces, evaluation of Parylene sheath probe designs *in vivo*, and development of sheath probe arrays to allow recording from large areas and multiple sites of interest. The fabrication process developed for manufacture of single probes is easily extended for the fabrication of probe arrays. This novel probe approach will also be investigated for a variety of neural

recording and stimulation applications in the central and peripheral nervous systems.

## Acknowledgements

The authors would like to thank Dr Victor Pikov and Kate Nelson at Huntington Medical Research Institutes (HMRI, Pasadena, CA 91105) for helpful discussions. The authors also thank Dr Donghai Zhu and members of the USC Biomedical Microsystems Laboratory for their support.

This work was sponsored by the Defense Advanced Research Projects Agency (DARPA) MTO under the auspices of Dr Jack Judy through the Space and Naval Warfare Systems Center, Pacific Grant/Contract No. N66001-11-1-4207.

## References

- 1 L. Galvani, *De viribus electricitatis in motu musculari commentarius, Ex Typographia Instituti Scientiarum Bologna*, 1791.
- 2 P. Gilgunn, R. Khilwani, T. Kozai, D. Weber, X. Cui, G. Erdos, O. Ozdoganlar and G. Fedder, presented in part at the 2012 IEEE 25th International Conference on Micro Electro Mechanical Systems (MEMS), Paris, France, 2012.
- 3 D. A. Robinson, *Proc. IEEE*, 1968, **56**, 1065–1071.
- 4 M. A. L. Nicolelis, D. Dimitrov, J. M. Carmena, R. Crist, G. Lehew, J. D. Kralik and S. P. Wise, *Proc. Natl. Acad. Sci. U. S. A.*, 2003, **100**, 11041.
- 5 K. Najafi and K. D. Wise, *IEEE J. Solid-State Circuits*, 1986, **21**, 1035–1044.
- 6 P. K. Campbell, K. E. Jones, R. J. Huber, K. W. Horch and R. A. Normann, *IEEE Trans. Biomed. Eng.*, 1991, **38**, 758–768.
- 7 V. S. Polikov, P. A. Tresco and W. M. Reichert, *J. Neurosci. Methods*, 2005, **148**, 1–18.
- 8 J. R. Capadona, D. J. Tyler, C. A. Zorman, S. J. Rowan and C. Weder, *MRS Bull.*, 2012, **37**, 581–589.
- 9 J. Subbaroyan, D. C. Martin and D. R. Kipke, *J. Neural Eng.*, 2005, **2**, 103.
- 10 P. R. Kennedy, *J. Neurosci. Methods*, 1989, **29**, 181–193.
- 11 P. R. Kennedy and R. A. Bakay, *NeuroReport*, 1998, **9**, 1707–1711.
- 12 P. R. Kennedy, R. A. Bakay and S. M. Sharpe, *NeuroReport*, 1992, **3**, 605–608.
- 13 P. R. Kennedy, S. S. Mirra and R. A. E. Bakay, *Neurosci. Lett.*, 1992, **142**, 89–94.
- 14 P. Kennedy, D. Andreasen, P. Ehirim, B. King, T. Kirby, H. Mao and M. Moore, *J. Neural Eng.*, 2004, **1**, 72.
- 15 J. Bartels, D. Andreasen, P. Ehirim, H. Mao, S. Seibert, E. J. Wright and P. Kennedy, *J. Neurosci. Methods*, 2008, **174**, 168–176.
- 16 F. H. Guenther, J. S. Brumberg, E. J. Wright, A. Nieto-Castanón, J. A. Tourville, M. Panko, R. Law, S. A. Siebert, J. L. Bartels, D. S. Andreasen, P. Ehirim, H. Mao and P. R. Kennedy, *PLoS One*, 2009, **4**, 1–11.
- 17 J. T. W. Kuo, B. J. Kim, S. A. Hara, C. Lee, C. A. Gutierrez, T. Hoang and E. Meng, presented in part at the Hilton Head 2012: Solid State Sensors, Actuators and Microsystems

- Workshop, Hilton Head Island, South Carolina, USA, June 3–7, 2012.
- 18 E. Meng, *Biomedical Microsystems*, CRC Press, 2010.
  - 19 E. Meng, X. Zhang and W. Benard, in *MEMS Materials and Processes Handbook*, ed. R. Ghodssi and P. Li, Springer, 2011, ch. 4, pp. 193–271.
  - 20 C. Shih, T. A. Harder and Y. C. Tai, *Microsyst. Technol.*, 2004, **10**, 407–411.
  - 21 Y. Nam, *MRS Bull.*, 2012, **37**, 566–572.
  - 22 A. V. Vasenkov, *J. Mol. Model.*, 2011, **17**, 3219–3228.
  - 23 C. A. Gutierrez and E. Meng, presented in part at the Transducers 2009, Denver, Colorado, USA, June 21–25, 2009.
  - 24 C. A. Gutierrez, Doctor of Philosophy Doctoral, University of Southern California, 2011.
  - 25 D. C. Rodger, A. J. Fong, W. Li, H. Ameri, A. K. Ahuja, C. Gutierrez, I. Lavrov, H. Zhong, P. R. Menon and E. Meng, *Sens. Actuators, B*, 2008, **132**, 449–460.
  - 26 H.-S. Noh, Y. Huang and P. J. Hesketh, *Sens. Actuators, B*, 2004, **102**, 78–85.
  - 27 C. A. Gutierrez, C. Lee, B. Kim and E. Meng, presented in part at the 16th International Solid-State Sensors, Actuators and Microsystems Conference (TRANSDUCERS), Beijing, China, 5–9 June 2011.
  - 28 S. Takeuchi, D. Ziegler, Y. Yoshida, K. Mabuchi and T. Suzuki, *Lab Chip*, 2005, **5**, 519–523.
  - 29 T. D. Y. Kozai and D. R. Kipke, *J. Neurosci. Methods*, 2009, **184**, 199–205.
  - 30 V. Pikov, personal communication.
  - 31 H. Noh, K. Moon, A. Cannon, P. J. Hesketh and C. Wong, *J. Micromech. Microeng.*, 2004, **14**, 625.
  - 32 J. P. Seymour, Y. M. Elkasabi, H. Y. Chen, J. Lahann and D. R. Kipke, *Biomaterials*, 2009, **30**, 6158–6167.
  - 33 R. Huang and Y. C. Tai, *Parylene to silicon adhesion enhancement*, 2009.
  - 34 S. F. Cogan, *Annu. Rev. Biomed. Eng.*, 2008, **10**, 275–309.
  - 35 H. Takahashi, J. Suzurikawa, M. Nakao, F. Mase and K. Kaga, *IEEE Trans. Biomed. Eng.*, 2005, **52**, 952–956.